Inorg. Chem. **2007**, *46*, 3603–3612

Synthesis and Spectroscopic Studies of Cyclometalated Pt(II) Complexes Containing a Functionalized Cyclometalating Ligand, 2-Phenyl-6-(1*H*-pyrazol-3-yl)-pyridine

Chi-Kin Koo,[†] Yu-Man Ho,[†] Cheuk-Fai Chow,[†] Michael Hon-Wah Lam,*[,†] Tai-Chu Lau,[†] and Wai-Yeung Wong[‡]

Department of Biology and Chemistry, City University of Hong Kong, 83 Tat Chee Avenue, Hong Kong SAR, China, and Department of Chemistry, Hong Kong Baptist University, Waterloo Road, Kowloon Tong, Hong Kong SAR, China

Received December 19, 2006

Three new luminescent cyclometalated Pt(II) complexes, [Pt(L)Cl] (**1**), [$Pt_2(L^-)_2$] (**2**), and [Pt(L)(PPh_3)]ClO_4 (**3**·ClO_4) (where HL = 2-phenyl-6-(1*H*-pyrazol-3-yl)-pyridine), were synthesized and characterized by X-ray crystallography. HL represents a new class of C,N,$N_{pyrazolyl}$ cyclometalating ligands containing a C_{phenyl}, a $N_{pyridyl}$, and a $N_{pyrazolyl}$ donor moiety, as well as a 1-pyrazolyl-NH, that can also be available for metal coordination and other chemical interactions. Complex **1** possesses intense intraligand transitions at 275–375 nm and moderately intense metal-to-ligand charge transfer (^{1}MLCT) (dπ(Pt) $\rightarrow$ π^*(L)) transition at 380–410 nm. The room temperature solid-state emission λ_{max} of **1** occurs at 580 nm and is attributable to the ^{3}MMLCT (dσ^*(Pt) $\rightarrow$ π^*(L)) transition. It also displays strong phosphorescence in acetonitrile solutions at room temperature with an emission λ_{max} at 514 nm, which can be tentatively assigned to the ^{3}MLCT (π^*(L) $\rightarrow$ dπ(Pt)) transition. Complex **1** can be deprotonated in organic solvents to yield a cycloplatinated dimer **2**, which shows a relatively high room-temperature luminescent quantum yield of 0.59 in DMF (λ_{max} = 509 nm). Substitution of the ancillary chloro-ligand in **1** by triphenylphosphine yields **3**, which also possesses a good room-temperature luminescent quantum yield of 0.52 in DMF (λ_{max} = 504 nm) and a better solubility in water. Complex **3** is synthesized to demonstrate the pH dependence of luminescent properties of this C,N,$N_{pyrazolyl}$ cyclometalated Pt(II) system. Such a pH response is ascribable to the protonation/deprotonation of the 1-pyrazolyl-NH on the C,N,$N_{pyrazolyl}$ cyclometalating ligand. The pK_a of the 1-pyrazolyl-NH in **3**, measured in 1:2 (v/v) aqueous DMF solutions, is approximately 4.0.

Introduction

The strategy of using specially designed ligand systems with one or two coordination moieties that serve to position a metal center close to an sp^2 C−H or sp^3 C−H for C−H bond activation and cyclometalation has been well explored to spawn a wide variety of cyclometalated complexes with interesting catalytic and photochemical/photophysical properties.[1] An array of coordination functionalities such as amino,[2,3] iminyl,[4,5] pyridyl,[6] pyrazolyl,[7] phosphinyl,[8] and thiol[9] have been utilized to hold and stabilize metal centers for cyclometalation. The nature of these coordination groups and their interactions with metal centers also bring about the varying chemical, spectroscopic, and photophysical properties of different cyclometalated systems. Of the many established cyclometalating ligands, the extensively π-conjugated bidentate and tridentate phenyl-substituted pyridine (the C,N and N,C,N motifs) and bipyridine (the C,N,N motif)

* To whom correspondence should be addressed. E-mail: bhmhwlam@cityu.edu.hk.
[†] City University of Hong Kong.
[‡] Hong Kong Baptist University.

(1) (a) Dehand, J.; Pfeffer, M. *Coord. Chem. Rev.* **1976**, *18*, 327. (b) Bruce, M. I. *Angew. Chem., Int. Ed. Engl.* **1977**, *16*, 73. (c) Wakatsuki, Y.; Tamazaki, H.; Grutsch, P. A.; Southanam, M.; Kutal, C. *J. Am. Chem. Soc.* **1985**, *107*, 8153. (d) Omae, I. *Organometallic Intramolecular-Coordination Compounds*; Elsevier Science: Amsterdam, New York, 1986. (e) Lewis, L. N. *J. Am. Chem. Soc.* **1986**, *108*, 143. (f) Craig, C. A.; Watts, R. J. *Inorg. Chem.* **1989**, *28*, 309. (g) Ryabov, A. D. *Chem. Rev.* **1990**, *90*, 403. (h) Chan, C. W.; Lai, T. F.; Che, C. M.; Peng, S. M. *J. Am. Chem. Soc.* **1993**, *115*, 11245. (i) Canty, A. J.; van Koten, G. *Acc. Chem. Res.* **1995**, *28*, 406. (j) Lu, W.; Mi, B.-X.; Chan, M. C. W.; Hui, Z.; Zhu, N. Y.; Lee, S.-T.; Che, C.-M. *Chem. Commun.* **2002**, 206. (k) Sun, W.; Zhu, H.; Barron, P. M. *Chem. Mater.* **2006**, *18*, 2602−2610.
(2) Terheijden, J.; van Koten, G.; Muller, F.; Grove, D. M.; Vrieze, K. *J. Organomet. Chem.* **1986**, *315*, 401−407.

10.1021/ic062439j CCC: $37.00
Published on Web 04/05/2007

as well as the related diphenyl-substituted pyridine (the C,N,C motif) systems have attracted substantial attention in recent years because of the outstanding photophysical properties of their cyclometalated complexes with d^6 and d^8 metal centers, such as Rh(III), Ir(III), Pt(II), and Au(III).[10] The open square planar geometry of their d^8 cyclometalated complexes is also a potential framework for substrate binding and chemosensing.[11,12] Among them, the tridentate C,N,N system is probably the most widely studied. For example, cyclometalated Pt(II) complexes of 6-phenyl-2,2′-bipyridine have found numerous applications in organic light-emitting diodes (OLEDs),[13] optical limiting devices,[1k] DNA and protein binding,[12] cation recognition,[14] and pH sensing.[15] While considerable efforts have been made to incorporate various functional substitutents on the C,N,N ligand to fine-tune its photochemical and photophysical properties,[13,16] attempts to develop new π-conjugated C,N,N cyclometalating ligand systems with donor groups other than bipyridine are scarce.[11]

We have recently synthesized a new tridentate π-conjugated C,N,$N_{pyrazolyl}$ cyclometalating ligand, 2-phenyl-6-(1*H*-pyrazol-3-yl)-pyridine (HL) (Figure 1), that contains a C_{phenyl}, a $N_{pyridyl}$, and a $N_{pyrazolyl}$ donor moiety as well as a 1-pyrazolyl-NH that can also be available for metal coordination and other chemical interactions.[17] The purpose of incorporating a C3-substituted pyrazolyl functionality into the C,N,N motif is twofold. First, electronic properties of the pyrazole ligand are closely linked to the acid−base properties of its 1-pyrazolyl-NH. Deprotonation of the 1-pyrazolyl-NH converts pyrazole from a weak π-accepting ligand to a strong π-donating ligand.[18] Thus, spectroscopic and photophysical properties of the C,N,$N_{pyrazolyl}$ cyclometalated system should be tunable by the acid−base environment of the media. Besides the regulation of electronic properties, the 1-pyrazolyl-NH is also a reactive site on the ligand that allows its cyclometalated complexes to take part in further chemical reactions/interactions. In most of the established tridentate cyclometalated systems, substitution of the liable ancillary ligand is the most common, if not the sole, approach for their functionalization as it is more convenient than the direct derivatization of the cyclometalating ligand, which usually involves tedious and multiplestep synthesis.[16] In the present C,N,$N_{pyrazolyl}$ system, both the ancillary and the cyclometalating ligands are available for easy derivatization. This should enable much greater flexibility in the functionalization and the incorporation of the cyclometalated complexes with desirable catalytic or spectroscopic properties into supramolecular devices and materials. It has to be pointed out that a number of established cyclometalated ligand systems have also made use of the pyrazolyl moiety as a donor group. However, to the best of our knowledge, they mainly involve N1-substituted pyrazoles which contain no 1-pyrazolyl-NH functionality and do not possess the special properties of the present C,N,$N_{pyrazolyl}$ ligand.[7,19]

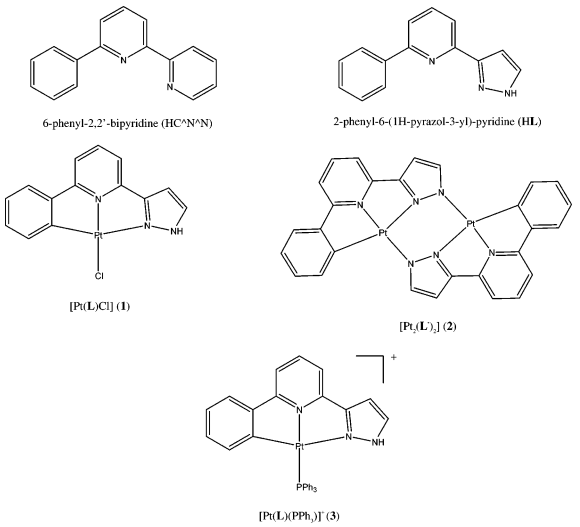

Figure 1. Cyclometalated C,N,N ligands and cycloplatinated complexes involved in this study.

(3) Gossage, R. A.; Ryabov, A. D.; Spek, A. L.; Stufkens, D. J.; van Beek, J. A. M.; van Eldik, R.; van Koten, G. *J. Am. Chem. Soc.* **1999**, *121*, 2488−2497.

(4) Muñoz, M. S.; García, B.; Ibeas, S.; Hoyuelos, F. J.; Peñacoba, I.; Navarro, A. M.; Leal, J. M. *New J. Chem.* **2004**, *28*, 1450−1456.

(5) Jacquot-Rousseau, S.; Khatyr, A.; Schmitt, G.; Knorr, M.; Kubicki, M.; Blacque, O. *Inorg. Chem. Commun.* **2005**, *8*, 610−613.

(6) (a) Constable, E. C.; Henney, R. P. G.; Leese, R. A.; Tocher, D. A. *J. Chem. Soc., Chem. Commun.* **1990**, 513. (b) Zucca, A.; Cinellu, M. A.; Pinna, M. V.; Stoccoro, S.; Minghetti, G.; Manassero, M.; Sansoni, M. *Organometallics* **2000**, *19*, 4295. (c) Kim, Y.-J.; Chang, X.; Han, J.-T.; Lim, M. S.; Lee, S. W. *Dalton Trans.* **2004**, 3699−3708. (d) Consorti, C. S.; Ebeling, G.; Rodembusch, F.; Stefani, V.; Livotto, P. R.; Rominger, F.; Quina, F. H.; Chang, Y.; Duppont, J. *Inorg. Chem.* **2004**, *43*, 530−536.

(7) Tamayo, A. B.; Garon, S.; Sajoto, T.; Djurovich, P. I.; Tsyba, I. M.; Bau, R.; Thompson, M. E. *Inorg. Chem.* **2005**, *44*, 8723−8732.

(8) (a) Weisman, A.; Gozin, M.; Kraatz, H.-B.; Milstein, D. *Inorg. Chem.* **1996**, *35*, 1792−1797. (b) Gusev, D. G.; Dolgushin, F. M.; Antipin, M. Y. *Organometallics* **2001**, *20*, 1001−1007. (c) van der Boom, M. E.; Milstein, D. *Chem. Rev.* **2003**, *103*, 1759−1792.

(9) Akaiwa, M.; Kanbara, T.; Fukumoto, H.; Yamamoto, T. *J. Organomet. Chem.* **2005**, *690*, 4192−4196.

(10) (a) Colombo, M. G.; Güdel, H. U. *Inorg. Chem.* **1993**, *32*, 3081. (b) Yersin, H.; Donges, D. *Top. Curr. Chem.* **2001**, *214*, 81−186. (c) Li, J.; Djurovich, P. I.; Alleyne, B. D.; Yousufuddin, M.; Ho, N. N.; Thomas, J. C.; Peters, J. C.; Bau, R.; Thompson, M. E. *Inorg. Chem.* **2005**, *44*, 1713−1727. (d) Lai, S. W.; Chan, M. C.; Peng, S. M.; Che, C. M. *Inorg. Chem.* **1999**, *38*, 4046−4055. (e) Yip, J. H. K.; Suwarno; Vittal, J. J. *Inorg. Chem.* **2000**, *39*, 3537−3543. (f) Cave, G. W. V.; Fanizzi, F. P.; Deeth, R. J.; Errington, W.; Rourke, J. P. *Organometallics* **2000**, *19*, 1355−1364. (g) Lu, W.; Chan, M. C.-W.; Cheung, K.-K.; Che, C.-M. *Organometallics* **2001**, *20*, 2477−2486. (h) Wong, K. M.-C.; Zhu, X.; Hung, L.-L.; Zhu, N.; Yam, V. W.-W.; Kowk, H.-S. *Chem. Commun.* **2005**, 2906−2908.

(11) (a) Chan, C.-W.; Lai, T.-F.; Che, C.-M.; Peng, S.-M. *J. Am. Chem. Soc.* **1993**, *115*, 11245−11253. (b) Kui, S. C. F.; Chui, S. S.-Y.; Che, C.-M.; Zhu, N. *J. Am. Chem. Soc.* **2006**, *128*, 8297−8309.

(12) Siu, P. K.-M.; Ma, D.-L.; Che, C.-M. *Chem. Commun.* **2005**, 1025−1027.

(13) Lu, W.; Mi, B.-X.; Chan, M. C. W.; Hui, Z.; Che, C.-M.; Lee, S.-T. *J. Am. Chem. Soc.* **2004**, *126*, 4958−4971.

(14) (a) Siu, P. K.-M.; Lai, S.-W.; Lu, W.; Zhu, N.; Che, C.-M. *Eur. J. Inorg. Chem.* **2003**, 2749−2752. (b) Yang, Q.-Z.; Wu, L.-Z.; Zhang, H.; Chen, B.; Wu, Z.-X.; Zhang; L.-P.; Tung, C.-H. *Inorg. Chem.* **2004**, *43*, 5195−5197.

(15) Wong, K.-H.; Chan, M. C.-W.; Che, C.-M. *Chem.—Eur. J.* **1999**, *5*, 2845−2849.

(16) (a) Neve, F.; Crispini, A.; Campagna, S. *Inorg. Chem.* **1997**, *36*, 6150−6151. (b) Sun, W.; Wu, Z.-X.; Yang, Q.-Z.; Wu, L.-Z.; Tung, C.-H. *Appl. Phys. Lett.* **2003**, *82*, 850−852.

(17) Koo, C.-K; Lam, B.; Leung, S.-K.; Lam, M. H.-W.; Wong, W.-Y. *J. Am. Chem. Soc.* **2006**, *128*, 16434−16435.

(18) Sullivan, B. P.; Salmon, D. J.; Meyer, T. J.; Peedin, J. *Inorg. Chem.* **1979**, *18*, 3369−3374.

(19) Tamayo, A. B.; Alleyne, B. D.; Djurovich, P. I.; Lamansky, S.; Tsyba, I. M.; Ho, N. N.; Bau, R.; Thompson, M. E. *J. Am. Chem. Soc.* **2003**, *125*, 7377−7387.

Table 1. Crystal Data and Structure Refinement Details for **1**, **2**, and **3**·ClO_4

	1	**2**	**3**·ClO_4
empirical formula	$C_{14}H_{10}ClN_3Pt$	$C_{28}H_{18}N_6Pt_2$	$C_{32}H_{25}ClN_3O_4PPt$
formula weight	450.79	828.66	777.06
temperature, K	293(2)	293(2)	293(2)
wavelength, Å	0.71073	0.71073	0.71073
crystal system	triclinic	monoclinic	monoclinic
space group	$P\bar{1}$	$P12_1/c1$	$P12_1/n1$
a, Å	8.1722(5)	10.5571(8)	15.1346(11)
b, Å	11.9826(7)	16.6276(12)	10.8111(8)
c, Å	13.6523(8)	19.5283(14)	17.5583(13)
α, deg	101.1730(10)	90	90
β, deg	98.6780(10)	103.9640(10)	93.0650(10)
γ, deg	100.9590(10)	90	90
volume, Å^3	1262.94(13)	3326.68(40)	2868.81(40)
Z	4	6	4
density (calculated), g cm^{-3}	2.371	2.482	1.799
absorption coefficient, mm^{-1}	11.308	12.634	5.084
F(000)	840	2304	1520
crystal dimensions, mm	0.32 × 0.26 × 0.24	0.20 × 0.18 × 0.18	0.32 × 0.15 × 0.13
θ range for data collection, deg	2.07−25.00	1.99−25.00	1.73−25.00
limiting indices	$-9 \le h \le 9$, $-14 \le k \le 11$, $-16 \le l \le 15$	$-7 \le h \le 1$, $-18 \le k \le 19$, $-23 \le l \le 20$	$-17 \le h \le 17$, $-12 \le k \le 12$, $-18 \le l \le 20$
reflections collected	6311	15842	13549
independent reflections (R_{int})	4379 (0.0197)	5851 (0.0316)	5037 (0.0307)
completeness to $q = 25.00°$, %	98.2	99.8	99.7
observed reflections [$I > 2\sigma(I)$]	3898	4802	4087
absorption correction		semiempirical form equivalents	
max and min transmission	1.0000 and 0.5069	1.0000 and 0.6813	1.0000 and 0.8137
refinement method		full-matrix least-squares equivalents	
data/restraints/parameters	4379/0/343	5851/0/487	5037/0/379
goodness of fit on F^2	1.036	1.050	1.064
final *R* indices [$I > 2\sigma(I)$]	R1 = 0.0207, wR2 = 0.0545	R1 = 0.0243, wR2 = 0.0547	R1 = 0.0297, wR2 = 0.0675
R indices (all data)	R1 = 0.0241, wR2 = 0.0561	R1 = 0.0382, wR2 = 0.0601	R1 = 0.0430, wR2 = 0.0726
largest different peak and hole, e Å^{-3}	0.996 and −1.010	1.085 and −1.581	1.328 and −1.373

In order to further explore the various special features of the C,N,$N_{pyrazolyl}$ cyclometalated system, a series of cycloplatinated complexes were synthesized in this work. The neutral [Pt(L)Cl] (**1**) is an analogue of the well-studied [Pt(C^N^N)Cl] (HC^N^N = 6-phenyl-2,2′-bipyridine) complex. In organic solvents, **1** can be deprotonated by an organic base and self-coupled to yield the neutral dimer, $[Pt_2(L^-)_2]$ (**2**). Substitution of the ancillary chloride ligand in **1** by PPh_3 yields the cationic $[Pt(L)(PPh_3)]^+$ (**3**), which possesses better water-solubility and is able to demonstrate the acid−base properties of the C,N,$N_{pyrazolyl}$ cyclometalated system. All the cyclometalated Pt(II) complexes synthesized in this study are strongly emissive in both the solid-state and solutions at room temperature, and their structures are characterized by X-ray crystallography.

Experimental Section

Materials and General Procedures. All starting materials, 2,6-dibromopyridine, *n*-butyl lithium (1.6 M in hexane), dimethylacetamide, phenylboronic acid, *N*,*N*-dimethylformamide dimethyl acetal, hydrazine hydrate, triethylamine, and K_2PtCl_4 were purchased from commercial sources and used as received unless stated otherwise. The solvents used for synthesis were of analytical grade. Diethyl ether was distilled from sodium-benzophenone, and acetonitrile was distilled from anhydrous calcium hydride prior to use. Acetonitrile for photophysical measurements was distilled over potassium permanganate and calcium hydride. 2-Acetyl-6-bromopyridine, 2-acetyl-6-phenylpyridine, and tetrakis(trisphenylphosphine)palladium were prepared according to literature methods.[20,21]

3-Dimethylamino-1-(6-phenyl-pyridine-2-yl)-propenone. A solution of 2-acetyl-6-phenylpyridine (2.00 g, 0.01 mol) in DMF dimethyl acetal (2.5 mL) was heated to reflux for 18 h. After concentration in vacuo, the resulting crude solid was recrystallized from $CHCl_3$/hexane to give a yellow crystalline product (1.84 g, yield: 72%). IR (KBr): $\nu = 1653$ cm^{-1} (s, C═O), 1545 cm^{-1} (s, C═C). ESI-MS: 253 $(M + 1)^+$. ^{1}H NMR (300 MHz, $CDCl_3$): δ 8.00−8.16 (m, 4H), 7.92−7.80 (m, 2H), 7.38−7.56 (m, 3H), 6.72 (d, 1H, $J = 12.6$ Hz), 3.22 (s, 3H), 3.06 (s, 3H). Elemental analysis calcd (%) for $C_{16}H_{16}N_2O_1$: C 76.16, H 6.39, N 11.10. Found: C 75.01, H 6.285, N 10.88.

2-Phenyl-6-(1*H*-pyrazol-3-yl)-pyridine (HL). A mixture of 3-dimethylamino-1-(6-phenyl-pyridine-2-yl)-propenone (1.75 g, 7 mmol), hydrazine hydrate (2.2 mL), and ethanol (1.7 mL) was heated to 65 °C with stirring for 1 h. The desired product was precipitated by the addition of water. The white precipitate was collected by filtration and washed with 3 × 20 mL of distilled water (1.5 g, yield: 98%). IR (KBr): $\nu = 3220$ cm^{-1} (s, N−H). ESI-MS: 222 $(M + 1)^+$, 443 $(M_2 + 1)^+$. ^{1}H NMR (300 MHz, DMSO-d_6): δ 13.13 (s, 1H), 8.26 (s, 2H), 7.70−8.04 (m, 4H), 7.40−7.62 (m, 3H), 6.99 (s, 1H). Elemental analysis calcd (%) for $C_{14}H_{11}N_3$: C 76.00, H 5.01, N 18.99. Found: C 75.95, H 5.08, N 18.89.

[Pt(L)Cl] (1). A mixture of the free ligand HL (0.20 g, 0.9 mmol) and K_2PtCl_4 (0.38 g, 0.9 mmol) in degassed glacial acetic acid (25 mL) was refluxed for 12 h to give a yellow precipitate. The precipitate was collected by filtration and washed with 10 mL of water, methanol, ethanol, and diethyl ether, respectively. Crystals suitable for X-ray crystallography were grown by slow evaporation of an acetone/MeOH solution (1.08 g, yield: 88%). IR (KBr): $\nu = 3264$ cm^{-1} (m, N−H). ^{1}H NMR (300 MHz, DMSO-d_6): δ 8.18 (1, 1H), 8.04 (t, 1H, $J = 8.1$ Hz), 8.82 (t, 2H, $J = 7.8$ Hz), 7.52 (d,

(20) Lötscher, D.; Rupprecht, S.; Stoeckli-Evans, H.; Zelewsky, A. *Tetrahedron: Asymmetry* **2000**, *11*, 4341−4357.
(21) Coulson, D. R. *Inorg. Synth.* **1990**, *28*, 107.

Scheme 1. Synthetic Pathway for the Preparation of the C,N,$N_{pyrazolyl}$ Ligand L[a]

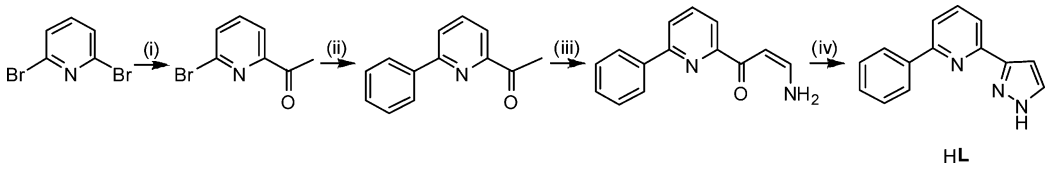

HL

[a] (i) *n*-BuLi, *N*,*N*-dimethylacetamide, Et_2O, −60 °C; (ii) phenylboronic acid in toluene, $Pd(PPh_3)_4$ (5% mol), K_2CO_3 in H_2O, reflux; (iii) DMF dimethyl acetal, reflux; (iv) N_2H_4, ethanol, 60 °C.

Scheme 2. Synthetic Pathway for the Preparation of the Dicycloplatinate Complex, **2**, from **1**

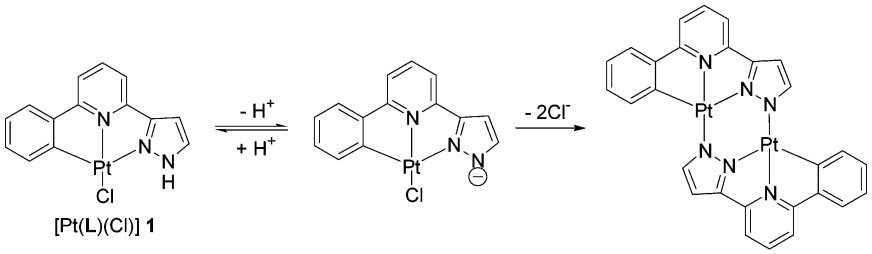

[Pt(L)(Cl)] **1** [$Pt_2(L^-)_2$] **2**

1H, J = 7.5 Hz), 7.56 (d, 1H, J = 7.5 Hz), 7.24 (s, 1H), 7.00−7.20 (m, 2H). Elemental analysis calcd (%) for $C_{14}H_{10}N_3PtCl$: C 37.30, H 2.236, N 9.321. Found: C 36.33, H 2.176, N 9.097.

[$Pt_2(L^-)_2$] (2). To a dichloromethane solution of **1** (0.02 g, 0.05mmol), a few drops of Et_3N were added. Crystals suitable for X-ray crystallography were obtained upon evaporation of the solvent within a few days (0.01 g, 50%). Elemental analysis calcd (%) for $C_{28}H_{18}N_6Pt_2 \cdot 1H_2O$: C 39.72, H 2.381, N 9.926. Found: C 39.84, H 2.434, N 9.882.

[Pt(L)(PPh_3)](ClO_4) (3·ClO_4). To an acetonitrile solution (50 mL) of **1** (0.1 g, 0.4 mmol) was added PPh_3 (0.26 g, 1.0 mmol). The mixture was stirred at room temperature for 12 h. A greenish-yellow suspension was obtained, and a methanolic solution of $LiClO_4$ (0.43 g, 4 mmol) was added. The mixture was stirred at room temperature for another 12 h, and the resulting clear yellow solution was filtered and evaporated to a minimal amount. The desired product was precipitated by the addition of diethyl ether as a bright greenish-yellow solid. The product was collected by filtration, washed with diethyl ether, and recrystallized by slow vapor diffusion of diethyl ether into an acetonitrile solution (0.15 g, yield: 87%). IR (KBr): ν = 3354 cm^{-1} (m, N−H), 1096 cm^{-1} (s, Cl═O). ESI-MS: 678 $(M + 1)^+$. ^1H NMR (300 MHz, DMSO-d_6): δ 11.24 (s, 1H), 8.26 (t, 1H, J = 7.8 Hz), 7.98−8.14 (m, 3H), 7.82−7.94 (m, 6H), 7.70−7.77 (d, 1H, J = 7.8 Hz), 7.52−7.70 (m, 9H), 7.34 (s, 1H), 7.04 (t, 1H, J = 6.9 Hz), 6.67 (t, 1H, J = 7.8 Hz), 6.31 (d, 1H, J = 7.5 Hz). Elemental analysis calcd (%) for $C_{32}H_{25}N_3O_4PtPCl \cdot {}^3/_4H_2O$: C 48.62, H 3.379, N 5.315. Found: C 47.65, H 3.325, N 5.344.

Physical Measurements and Instrumentation. Infrared spectra in the range 500−4000 cm^{-1} in KBr plates were recorded on a Perkin-Elmer model FTIR-1600 spectrometer. UV−vis spectra were measured on a Hewlett-Packard 8452A ultraviolet visible diode array spectrophotometer. Emission spectra were recorded using a Horiba FluoroMax-3 spectrofluorimeter with 5 nm slit width and 0.5 s integration time. Low-temperature (77 K) emission spectra were collected in 5-mm diameter quartz tubes which were placed in a liquid-nitrogen Dewar equipped with quartz windows. ^1H NMR spectra were recorded using a Varian YH300 300 MHz NMR spectrometer. Electrospray (ESI) mass spectra were measured by a PE SCIEX API 365 LC−MS/MS system. Elementary analyses were performed on a Vario EL elementary analyzer.

Sample and standard solutions were degassed with at least three freeze−pump−thaw cycles. Emission quantum yields were measured by the method of Demas and Crosby[22] with $[Ru(bpy)_3](PF_6)_2$ in degassed acetonitrile as the standard (ϕ_r = 0.062). Lifetime measurements were performed by a nitrogen laser (Spectra Physics) at 337 nm with the maximum power of 15 mW. The luminescence was dispersed by a monochromator and was detected using a cooled R636-10 Hamamastu photon-multiplier (PMT) in combination with a lock-in amplifier system. The decay spectra were monitored by a HP54522A 500 MHz oscilloscope.

Crystal Structure Determination. Crystallographic data for complexes **1, 2**, and **3**·ClO_4 were tabulated in Table 1. All intensity data were collected at 293 K on a Bruker Axs SMART 1000 CCD area detector using graphite-monochromated Mo Kα radiation (λ = 0.710 73 Å). All collected frames were processed with the software SAINT,[23] and absorption correction was applied (SADABS[24]) to the collected reflections. The structure of the complex was solved by direct methods (SHELXTL[25]) in conjunction with standard difference Fourier syntheses. All non-hydrogen atoms were assigned with anisotropic displacement parameters. The hydrogen atoms were generated in their idealized positions and allowed to ride on the respective carbon atoms.

Results and Discussion

Synthesis and Characterization. The C,N,$N_{pyrozolyl}$ cyclometalating ligand, HL, was prepared by a modified literature procedure outlined in Scheme 1. 2-Acetyl-6-bromopyridine, obtained from 2,6-dibromopyridine via lithiation with *n*-butyl lithium and dimethylacetamide, was converted to 2-acetyl-6-phenylpyridine by a palladium catalyzed Suzuki cross-coupling reaction with phenylboronic acid. The ketone was then converted into the intermediate, 3-dimethylamino-1-(6-phenyl-pyridine-2-yl)-propenone, by refluxing with *N*,*N*-dimethylformamide dimethyl acetal.[26]

(22) Demas, J. N.; Crosby, G. A. *J. Phys. Chem.* **1971**, *75*, 991.
(23) *SAINT Reference Manual*; Siemens Energy and Automation: Madison, WI, 1994−1996.
(24) Sheldrick, G. M. *SADABS, Empirical Absorption Correction Program*; University of Göttingen: Göttingen, Germany, 1997.
(25) Sheldrick, G. M. *SHELXTL Reference Manual*, version 5.1; Siemens: Madison, WI, 1997.
(26) (a) Lin, Y.-I.; Lang, S. A. *J. Heterocycl. Chem.* **1977**, *14*, 345−347. (b) Amoroso, A. J.; Cargill Thompson, A. M. W.; Jeffery, J. C.; Jones, P. L.; McCleverty, J. A.; Ward, M. D. *J. Chem. Soc., Chem. Commun.* **1994**, 2751.

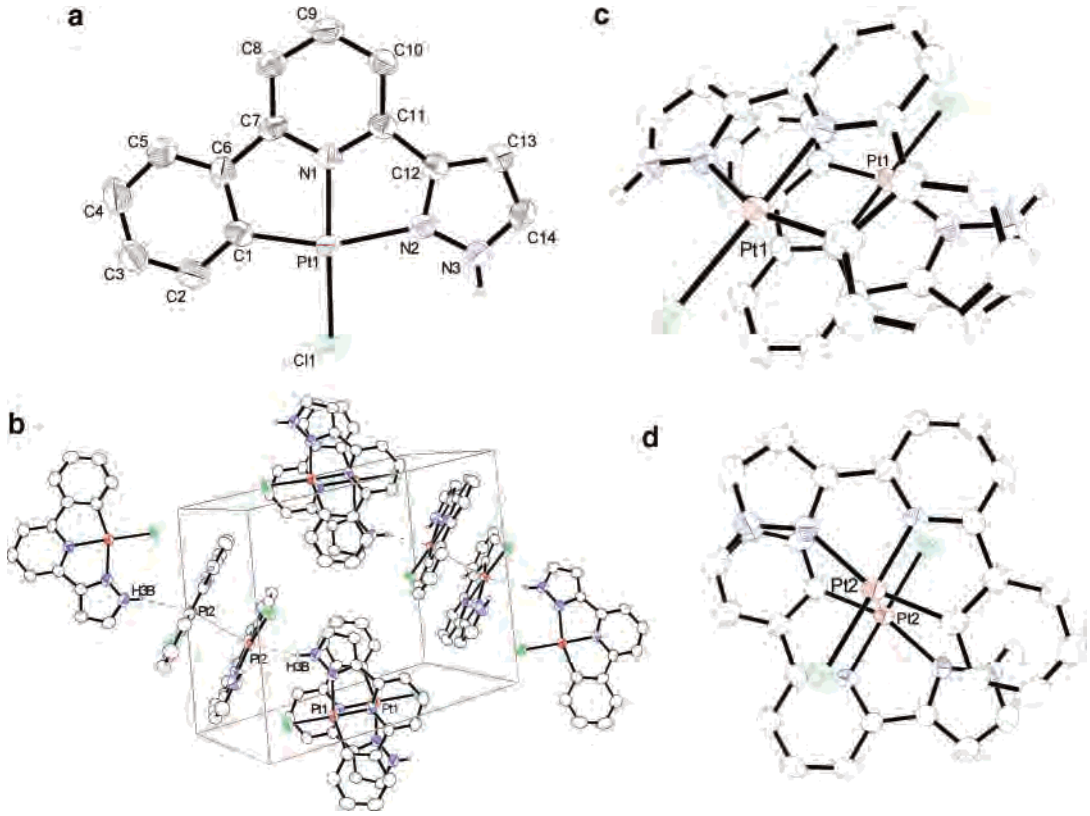

Figure 2. (a) Molecular structure of [Pt(L)Cl] (**1**) with the numbering scheme adopted. Thermal ellipsoids are shown at the 50% probability level. (b) Crystal packing mode of [Pt(L)Cl] (**1**). (c) Dimeric stacking of [Pt(L)Cl] via $\pi-\pi$ interaction. (d) Dimeric stacking [Pt(L)Cl] via Pt−Pt interaction.

This intermediate was isolated and purified by recrystallization and was transformed to HL by hydrazine.

The neutral cycloplatinated complex [Pt(L)Cl] (**1**) was obtained in over 80% yield by refluxing HL and K_2PtCl_4 in glacial acetic acid[27] for 12 h. Longer reaction time lowers the yield significantly. Addition of a few drops of triethylamine to a suspension of **1** in dichloromethane caused the immediate dissolution of the cyclometalated complex. Slow evaporation of the resulting solution gave the crystalline product $[Pt_2(L^-)_2]$ (**2**) which was characterized to be a neutral dimeric cycloplatinated $C,N,N_{pyrazolyl}$ complex. The formation of **2** is believed to be induced by the deprotonation of the 1-pyrazolyl-NH of the $C,N,N_{pyrazolyl}$ ligand of **1** followed by the coupling of two cycloplatinated units via substitution of the labile ancillary chloride ligands by the anionic pyrazolyl moieties of each other (Scheme 2). The labile chloride ligand in **1** can also be substituted by triphenylphosphine in acetonitrile to generate the cationic cycloplatinated complex $[Pt(L)(PPh_3)]^+$ (**3**).

All the Pt(II) $C,N,N_{pyrazolyl}$ cyclometalated complexes **1**, **2**, and **3**·ClO_4 were characterized by ^1H NMR, IR spectroscopy, and elementary analysis. Structures of these complexes were revealed by X-ray crystallography.

Crystal Structure of [Pt(L)Cl] (1). Single crystals of **1** that are suitable for X-ray crystallography were grown by slow evaporation of solvent from a concentrated acetone/methanol solution. Figure 2a shows the perspective view of **1**. Selected bond lengths and angles are listed in Table 2. The coordinate geometry of the Pt atom is a distorted square planar configuration with a C(1)−Pt(1)−N(2) angle of 160.34(17)°. Bond distances of Pt(1)−C(1), Pt(1)−N(1), and Pt(1)−N(2) are 1.992(2), 1.963(4), and 2.113(4) Å, respectively, which are all comparable to the analogous [Pt(C^N^N)Cl][28] (HC^N^N = 6-phenyl-2,2′-bipyridine). However, instead of forming a continuous chain linked by Pt−Pt interaction as in [Pt(C^N^N)Cl], the crystal lattice of **1** is packed by two kinds of alternating, orthogonally arranged dimeric [Pt(L)Cl] units (Figure 2b). In both kinds of arrangement, the [Pt(L)Cl] units are planar and parallel to each other. Figure 2c shows the configuration of one of the dimeric arrangements. The two [Pt(L)Cl] units are stacked in a head-to-tail fashion with a Pt−Pt distance of 4.638(3) Å, suggesting no metal−metal interaction. The two [Pt(L)-

Table 2. Selected Bond Lengths (Å) and Angles (deg) of Complex [Pt(L)Cl] (**1**)

Pt(1)−C(1)	1.992(5)	Pt(1)−N(1)	1.963(4)
Pt(1)−N(2)	2.113(4)	Pt(1)−Cl(1)	2.310(1)
Pt(1)−Pt(1)	4.638(3)	Pt(2)−Pt(2)	3.329(2)
Pt(2)−H(3b)	2.553(1)	Cl (1)−H(24A)	2.871(2)
C(1)−Pt(1)−N(1)	82.15(19)	C(1)−Pt(1)−Cl(1)	99.43(15)
N(1)−Pt(1)−N(2)	78.19(15)	N(2)−Pt(1)−Cl(1)	100.23(1)
N(1)−Pt(1)−Cl(1)	178.42(12)	C(1)−Pt(1)−N(2)	160.34(17)

(27) Cardenas, D. J.; Echavarren, A. M.; Ramirez de Arellano, M. C. *Organometallics* **1999**, *18* (17), 3337−3341.

(28) Hofmann, A.; Dahlenburg, L.; Eldik, R. *Inorg. Chem.* **2003**, *42*, 6528−6538.

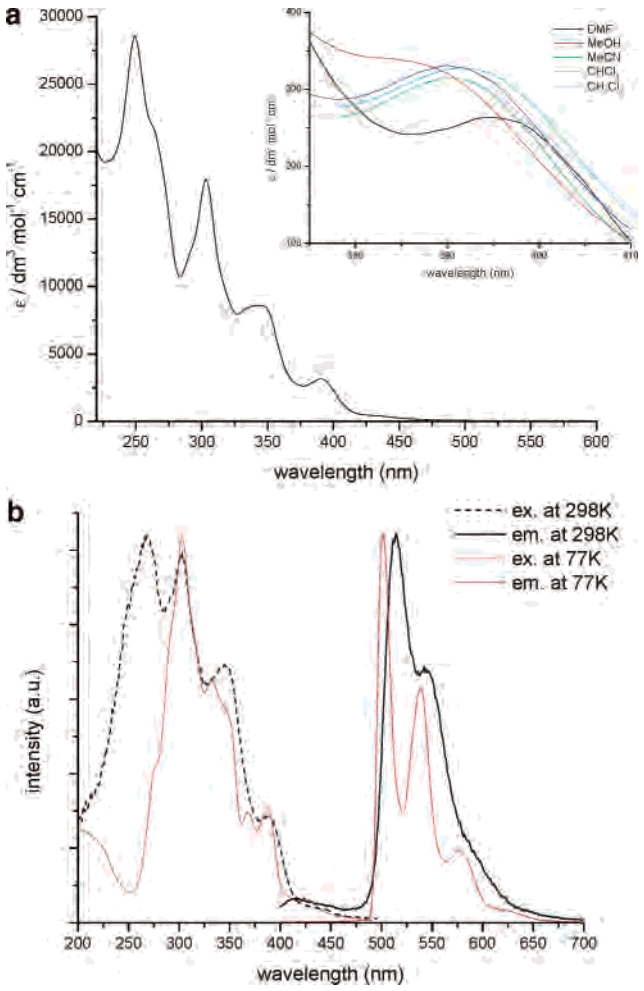

Figure 3. (a) UV−vis absorption spectrum of [Pt(L)Cl] (**1**) in acetonitrile at 298 K. The inset shows the solvent dependence of the lower energy absorption band at 380−410 nm. (b) Normalized excitation and emission spectra of [Pt(L)Cl] (**1**) in acetonitrile (2.5×10^{-5} M) at 298 K and in an alcoholic glassy solution (5:1:4 DMF/MeOH/EtOH) at 77 K.

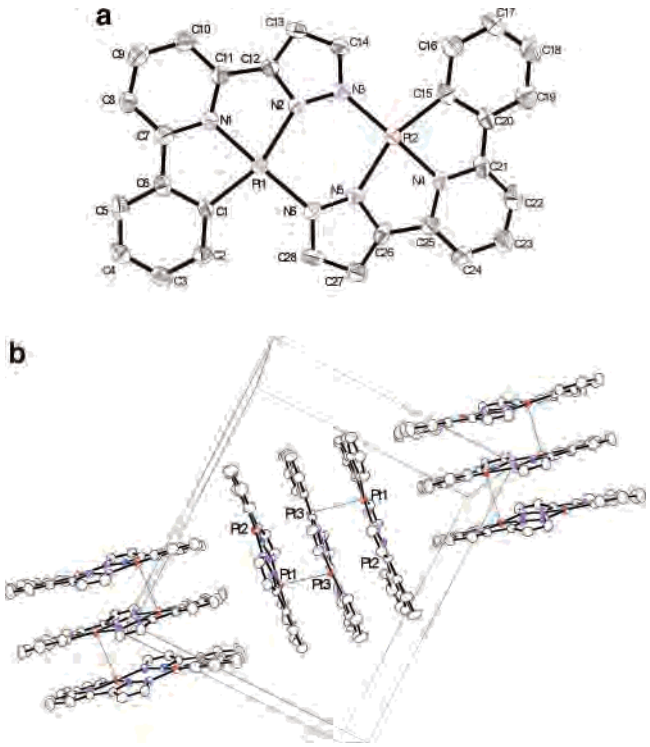

Figure 4. (a) Molecular structure of $[Pt_2(L^-)_2]$ (**2**) with the numbering scheme adopted. Thermal ellipsoids are shown at the 50% probability level. (b) Crystal packing of $[Pt_2(L^-)_2]$ (**2**).

Cl] are likely to be held together by a weak $\pi-\pi$ interaction between their C,N,$N_{pyrazolyl}$ ligands which is indicated by the interplanar separations of 3.445(8)−3.801(7) Å. Figure 2d shows the configuration of the other type of dimeric arrangement. While the two [Pt(L)Cl] units are also stacked in a head-to-tail fashion, the Pt−Pt separation is only 3.329(2) Å, suggesting the presence of Pt−Pt interactions. On the other hand, as indicated by the poor overlapping between the aromatic moieties on the ligand, $\pi-\pi$ stacking interaction between the C,N,$N_{pyrazolyl}$ ligands is absent. These two kinds of dimeric units are arranged perpendicular to each other with the 1-pyrazolyl-NH on the C,N,$N_{pyrazolyl}$ ligands of the $\pi-\pi$ stacked dimers interacting with the Pt(II) centers of the Pt−Pt interacted dimers. The distance of $N_{pyrazolyl}H\cdots Pt$ is approximately 2.55 Å.

Spectroscopic and Luminescent Properties of 1. Figure 3a shows the electronic transition spectra of **1**. Detailed spectroscopic and luminescent data are summarized in Table 3. In acetonitrile, **1** exhibits intense absorption bands at approximately 275−375 nm with extinction coefficients (ϵ) of the order of 10^4 dm^3 mol^{-1} cm^{-1} and a less intense band at approximately 380−410 nm with ϵ of the order of 10^3 dm^3 mol^{-1} cm^{-1}. With reference to previous spectroscopic studies of its analogous [Pt(C^N^N)Cl], absorption bands at 275−375 nm most probably originate from the intraligand (π(L) → π*(L)) transitions while the lower energy absorption band at 380−410 nm can be assigned to the spin-allowed singlet dπ(Pt) → π*(L) metal-to-ligand charge transfer (^{1}MLCT) transition. The λ_{max} value of the lower energy band is solvent dependent and shifts from 384 nm in methanol to 392 nm in dichloromethane. This supports the assignment that the absorption band arises from a charge-transfer transition. The ^{1}MLCT absorption band obeys Beer's law in the range from 10^{-5} to 10^{-4} mol dm^{-3} suggesting no dimerization or oligomerization of the complex within this concentration range. The absorption shoulder at 420−475 nm is tentatively assigned to the spin-forbidden ^{3}MLCT (dπ(Pt) → π*(L)) transition.

Complex **1** exhibits strong luminescence in both solid-state and solutions at room temperature (Table 4). In acetonitrile at 298 K, **1** gives a poorly resolved emission profile with λ_{max} at approximately 514 nm (τ = 0.57 μs; ϕ = 0.14) (Figure 3b). At 77 K, an alcoholic glass of **1** shows a well-resolved vibronic structured emission profile at 475−660 nm with spacing of approximately 1300 cm^{-1} which can be correlated to the skeletal vibrational frequency of the C,N,$N_{pyrazolyl}$ ligand. The large Stoke's shift and relatively long observed emission lifetime suggest that the emission originates from a spin-forbidden triplet excited state. Except in DMF, emission of **1** shows only minor solvent dependence at room temperature. The emission λ_{max} shifts from 511 nm in methanol to 516 nm in dichloromethane (λ_{max} shifts to 522 nm in DMF). With reference to [Pt(C^N^N)Cl], the

Table 3. Room-Temperature UV−Visible Absorption and Emission Data of the Cycloplatinated Complexes **1**, **2**, and **3**·ClO_4 in Various Solvents

complex	medium	UV−vis absorption at 298 K λ/nm (ϵ_{max}/dm^3 mol^{-1} cm^{-1})	emission at 298 K λ_{max}/nm	emission at 77 K (frozen state) λ_{max}/nm
[Pt(L)Cl] (**1**)	DMF	306 (16104), 351 (9194), 394 (2633)	522	504
	MeOH	247 (36913), 263 (26982), 303 (22168), 335 (11603), 386 (3368)	511	504
	MeCN	249 (28585), 303 (17936), 345 (8598), 390 (3150)	514	502
	$CHCl_3$	252 (29783), 306 (18843), 343 (9903), 390 (3315)	514	503
	CH_2Cl_2	251 (31078), 305 (19259), 341 (9397), 392 (3278)	516	513
[Pt2(L^-)$_2$] (**2**)	DMF	310 (16290), 338 (13521), 350 (13235), 372 (13100), 385−415 (∼2500), 415−475 (∼500)	509	500
[Pt(L)(PPh_3)](ClO_4) (**3**·ClO_4)	DMF	332 (12693), 342 (11460), 360 (5543), 390−470 (∼580)	509	501
	MeOH	328 (9922), 344 (8339), 380−470 (∼400)	504	496
	MeCN	328 (10168), 342 (8789), 370−470 (∼530)	504	516

Table 4. Solid and Solution State Emission Data

		emission in fluid solution (at 298 K)			
complex	solid state emission λ_{max}/nm	λ_{max}/nm[a]	τ_o/μs[b]	Φ_{lum}[c]	emission in glass (at 77 K)[d] λ_{max}/nm
Pt(L)Cl (**1**)	550, 580	514	0.57	0.14	501
$Pt_2(L^-)_2$ (**2**)	636	509	3.65	0.59	503
[Pt(L)(PPh_3)](ClO_4) (**3**·ClO_4)	536	504	1.00	0.52	502

[a] Measured in acetonitrile (2.5×10^{-5} M), except **2** in DMF. [b] Measured in acetonitrile (2.5×10^{-5} M), with excitation λ at 355 nm (except **2** in DMF). [c] Use of $Ru(bpy)_3(PF_6)_2$ in degassed acetonitrile at 298K ($\phi_r = 0.062$) as reference. [d] Measured in 5:1:4 DMF/MeOH/EtOH (v/v) glassy solution.

emission peak of **1** at approximately 510 nm can be tentatively assigned to the ^{3}MLCT (π^*(L) → dπ(Pt)) transition. Compared to [Pt(C^N^N)Cl], the ^{3}MLCT emission of **1** is blue-shifted (λ_{max} of the ^{3}MLCT emission of [Pt(C^N^N)Cl] in acetonitrile at 298 K is 550 nm). This is probably due to the more energetic π^*(L) of the C,N,$N_{pyrazolyl}$ ligand which increases the ^{3}MLCT energy gap.

Effect of Deprotonation of 1. The 1-pyrazolyl-NH in the C,N,$N_{pyrazolyl}$ cyclometalating ligand of **1** is expected to be deprotonated under basic conditions, which should set off significant changes in its spectroscopic and photophysical properties. However, attempts to carry out spectroscopic or luminescence pH titration of **1** in aqueous−organic media were unsuccessful due to the poor solubility of the deprotonation product. This led us to investigate the possibility of isolating the deprotonated species in an organic solvent. It was subsequently observed that addition of triethylamine to a dichloromethane suspension of **1** causes the immediate dissolution of the deprotonation product. Slow evaporation of the dichloromethane solvent gives the crystalline product **2**. While **2** is crystallized from dichloromethane, it cannot be dissolved back into dichloromethane or most of the other organic solvents, except DMF in which **2** shows a limited solubility.

Crystal Structure of [$Pt_2(L^-)_2$] (2). X-ray crystallographic analysis reveals that complex **2** is a neutral dimeric cycloplatinated complex containing two deprotonated [C,N,$N_{pyrazolyl}^-$] ligands, [$Pt_2(L^-)_2$] (Figure 4a), and its selected bond lengths and angles are listed in Table 5. The

Table 5. Selected Bond Lengths (Å) and Angles (deg) for Complex [$Pt_2(L^-)_2$] (**2**)

Pt(1)−C(1)	2.013(6)	Pt(1)−N(1)	1.964(5)
Pt(1)−N(2)	2.098(5)	Pt(1)−N(6)	2.020(5)
Pt(2)−C(15)	2.014(7)	Pt(2)−N(4)	1.969(5)
Pt(2)−N(5)	2.095(6)	Pt(2)−N(3)	2.014(5)
Pt(1)−Pt(3)	3.479(1)	Pt(2)−Pt(3)	3.820(1)
Pt(2)−H(5A)	2.794(1)		
C(1)−Pt(1)−N(1)	80.72(22)	C(1)−Pt(1)−N(6)	101.19(22)
N(1)−Pt(1)−N(2)	78.87(22)	N(2)−Pt(1)−N(6)	99.30(21)
N(1)−Pt(1)−N(6)	177.88(22)	C(1)−Pt(1)−N(2)	159.04(23)
C(15)−Pt(2)−N(4)	80.82(23)	C(15)−Pt(2)−N(3)	101.34(23)
N(4)−Pt(2)−N(5)	78.82(22)	N(5)−Pt(2)−N(3)	99.08(21)
N(4)−Pt(2)−N(3)	175.17(22)	C(15)−Pt(2)−N(5)	159.59(24)

coordinate geometry of each Pt atom is a distorted square planar with the averaged C_{phenyl}−Pt−$N_{pyrazolyl}$ angle of 159.3°. The averaged Pt−C_{phenyl}, Pt−$N_{pyridyl}$, and Pt−$N_{pyrazolyl}$ bond lengths in the dimer are 2.014, 1.967, and 2.097 Å, respectively. The two Pt(II) centers are linked by the deprotonated pyrazolyl moiety of the [C,N,$N_{pyrazolyl}^-$] ligands to form a six-member ring configuration with the average Pt−$N_{pyrazolyl}^-$ bond length of 2.017 Å.

Crystal packing of **2** shows an interesting "trimers-of-dimers" arrangement (Figure 4b) analogous to the "oligomers-of-dimers" crystal packing of the d^{10} Cu(I) and Ag(I) complexes of 1*H*-[2,2′]bipyridinyl-6-one and 1*H*-[1,10]-phenanthrolin-2-one recently reported by Zhang et al.[29] Each of the trimeric stack of three [$Pt_2(L^-)_2$] units is orthogonal

(29) Zhang, J. P.; Wang, Y. B.; Huang, X. C.; Lin, Y. Y.; Chen, X. M. *Chem.−Eur. J.* **2005**, *11*, 552−561.

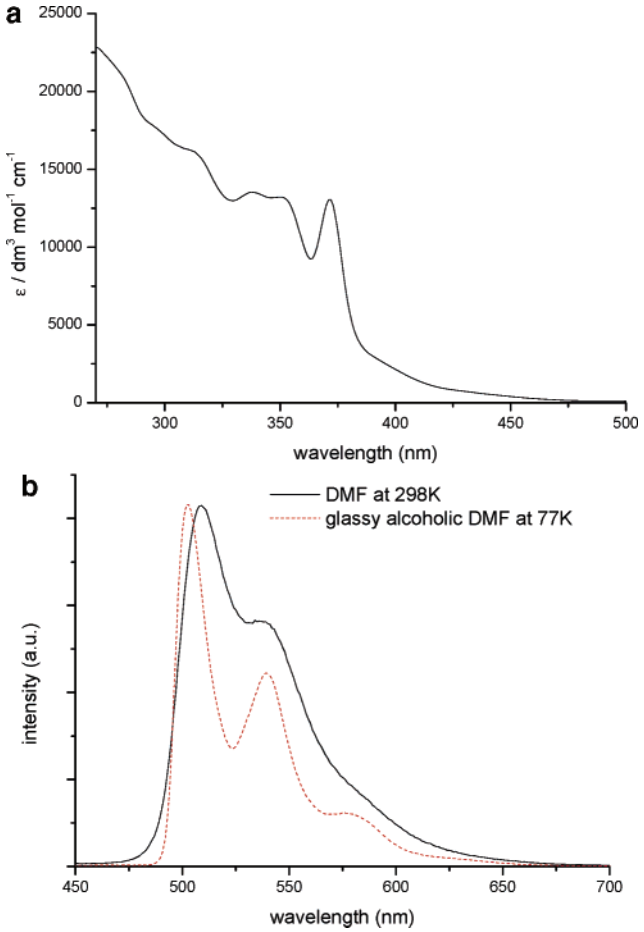

Figure 5. (a) UV−vis absorption spectrum of $[Pt_2(L^-)_2]$ (**2**) in DMF solution at 298 K. (b) Normalized emission spectra of $[Pt_2(L^-)_2]$ (**2**) in DMF (2.5×10^{-5} M) at 298 K and in an alcoholic glassy solution (5:1:4 DMF/MeOH/EtOH) at 77 K. (Excitation $\lambda = 355$ nm.)

to its adjacent stacks. Within each stack, the two Pt(II) centers in the middle $[Pt_2(L^-)_2]$ unit are interacting with different Pt(II) centers on its two sides. The distance between the Pt(II) centers with Pt−Pt interaction is approximately 3.479(1) Å while that between Pt(II) centers without Pt−Pt interaction is approximately 3.820(1) Å. The interplanar distance of 3.559(10)−3.895(11) Å indicates weak $\pi-\pi$ interaction between adjacent $[Pt_2(L^-)_2]$ units. In other words, the stacks of $[Pt_2(L^-)_2]$ dimers are held by both metal−metal and ligand−ligand interactions. Adjacent stacks are held by a weak $C_{aromatic}$−H···Pt interaction with a distance of 2.794(1)Å.

Spectroscopic and Luminescent Properties of 2. Because of the low solubility in common organic solvents, absorption and emission spectra of **2** can only be recorded in DMF (Figure 5a). Complex **2** exhibits an intense and sharp absorption band centered at 372 nm which can be assigned to the spin-allowed ^{1}MLCT ($d\pi(Pt) \rightarrow \pi^*(L)$) transition. In reference to complex **1**, the intense high-energy absorption bands at 275−360 nm and the weak lower energy absorption tail at 385−470 nm are assigned to the intraligand ($\pi(L) \rightarrow \pi^*(L)$) and the spin-forbidden ^{3}MLCT ($d\pi(Pt) \rightarrow \pi^*(L)$) transition, respectively.

Complex **2** shows similar luminescence properties compared to its precursor **1**. Upon 355 nm excitation at 298 K, a DMF solution of **2** displays a characteristic greenish-yellow emission with λ_{max} at 509 nm ($\tau = 3.65$ μs; $\phi = 0.59$) (Figure 5b) while the solid-state emission shows a poorly resolved emission profile centered at 636 nm. The room-temperature solution emission is attributable to the ^{3}MLCT ($d\pi^*(Pt) \rightarrow \pi^*(L)$) transition while the solid-state emission can be assigned to the excimeric ^{3}MMLCT ($d\sigma^*(Pt) \rightarrow \pi^*(L)$) transition due to the presence of both Pt−Pt and $\pi-\pi$ interaction observed in the solid-state crystal packing. The relatively long emission lifetime and the outstanding luminescent quantum yield of **2** are probably due to its rigid molecular structure.

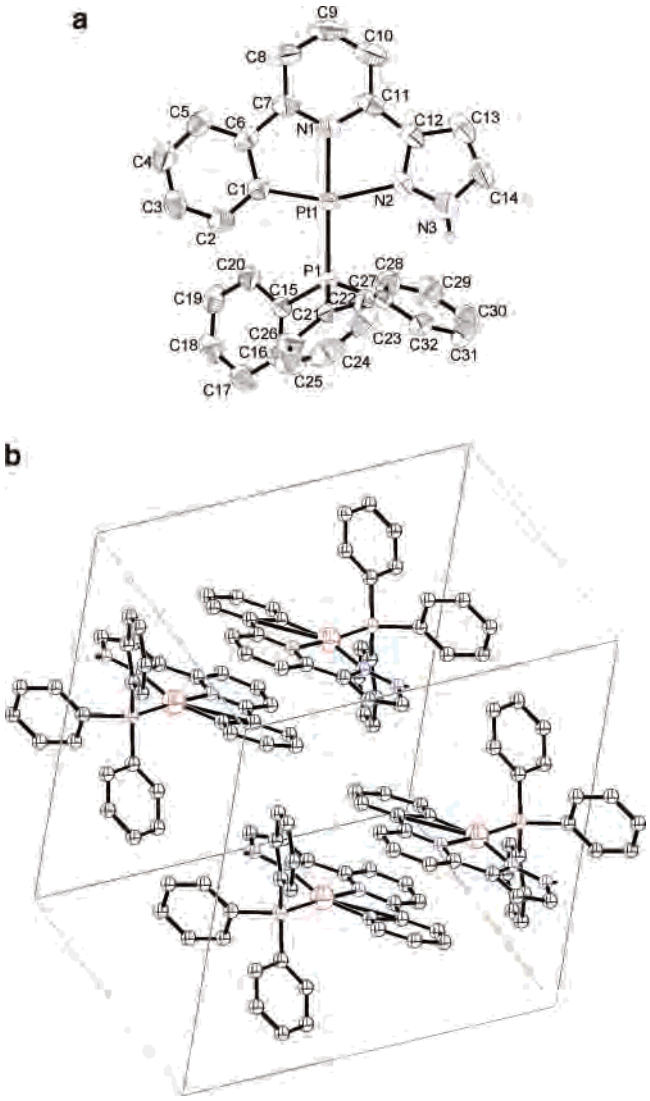

Figure 6. (a) Molecular structure of $[Pt(L)(PPh_3)]^+$ (**3**) with the numbering scheme adopted. Thermal ellipsoids are shown at the 50% probability level. (b) Crystal packing of $[Pt(L)(PPh_3)]^+$ (**3**).

Crystal Structure of $[Pt(L)(PPh_3)](ClO_4)$ ($3\cdot ClO_4$). Figure 6a shows the perspective view of the cationic complex **3**, and its selected bond lengths and angles are listed in Table 6. The Pt(II) center adopts a slightly distorted square planar geometry as in its precursor **1**. The C(1)−Pt(1)−N(2) angle is 157.41(19)°. The Pt(1)−P(1) bond length of 2.242(1) in **3** is comparable to that of the analogous cyclometalated complex $[Pt(C^N^N)(PPh_3)]^+$.[27] Figure 6b shows the crystal

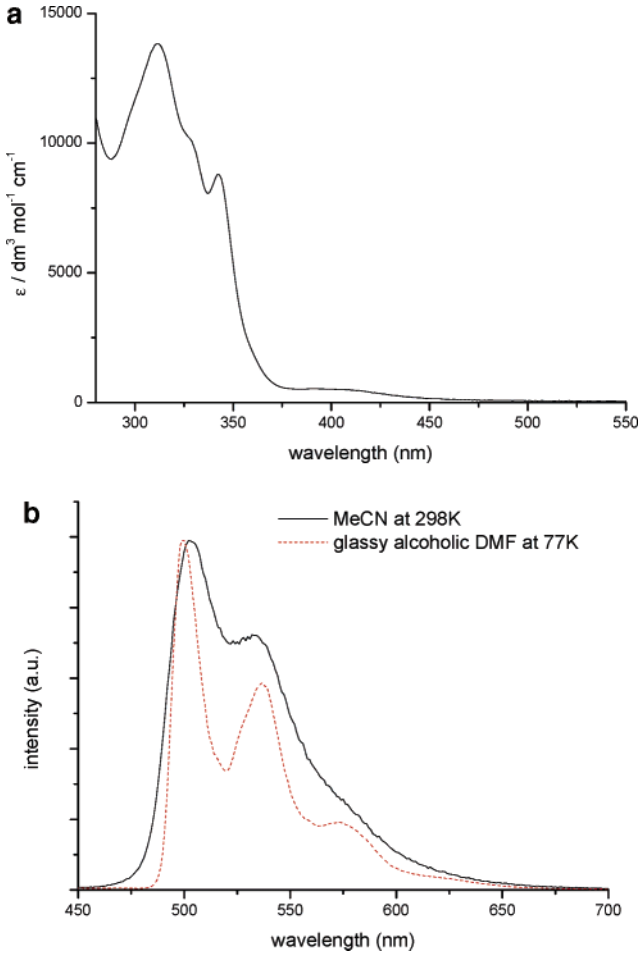

Figure 7. (a) UV−vis absorption spectrum of $[Pt(L)(PPh_3)]^+$ (**3**·ClO_4) in acetonitrile at 298 K. (b) Normalized emission spectra of $[Pt(L)(PPh_3)]^+$ (**3**)·ClO_4 in acetonitrile (2.5×10^{-5} M) at 298 K and in an alcoholic glassy solution (5:1:4 DMF/MeOH/EtOH) at 77 K. (Excitation $\lambda = 320$ nm.)

packing of **3**. Because of the presence of the bulky PPh_3 ligand which hinders the approach of the two Pt(II) centers, no Pt−Pt interaction is observed between adjacent $[Pt(L)(PPh_3)]^+$ units, and the shortest Pt−Pt distance is 5.890(3) Å. $[Pt(L)(PPh_3)]^+$ units are paired in a head-to-tail fashion with interplanar separation between the $C,N,N_{pyrazolyl}$ ligands in the range of 3.441(9)−3.952(9) Å indicating the presence of weak $\pi-\pi$ interactions. However, only the phenyl−pyridyl moieties of the cyclometalated ligand were involved in the stacking.

Spectroscopic and Luminescent Properties of 3·ClO_4. Absorption and emission spectra of **3** in acetonitrile are depicted in Figure 7. Similar to its precursor, **1**, the intense absorption bands in the range of 220−335 nm with ϵ of the order of 10^4 dm^3 mol^{-1} cm^{-1} are attributable to the intraligand ($\pi(L) \rightarrow \pi^*(L)$) transitions. The absorption band at approximately 345 nm can be assigned to the ^{1}MLCT ($d\pi(Pt) \rightarrow \pi^*(L)$) transition. In addition to these well-defined absorption bands, the solution spectrum also displays an absorption tail at 370−450 nm and is attributed to the ^{3}MLCT ($d\pi(Pt) \rightarrow \pi^*(L)$) transition.

Upon 355 nm excitation at room temperature, the cationic complex **3** exhibits strong solution luminescence at λ_{max} 504 nm ($\tau = 1.0$ μs; $\phi = 0.52$) in acetonitrile which can be

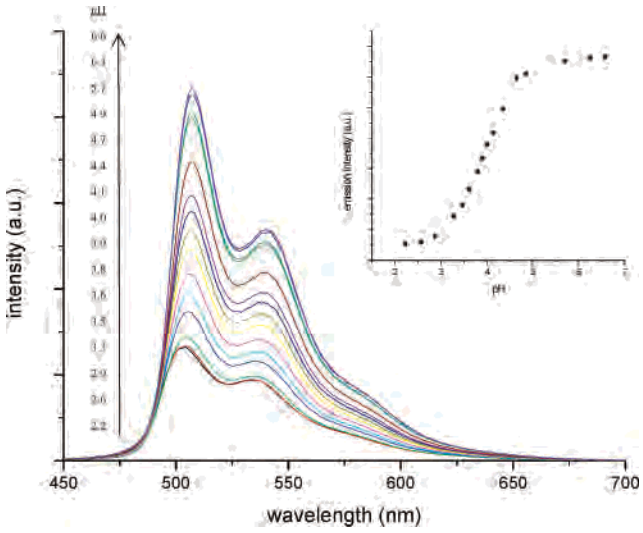

Figure 8. Emission spectra of $[Pt(L)(PPh_3)]^+$ (**3**·ClO_4) in 2:1 (v/v) DMF/buffered H_2O (3×10^{-5} M) at different pH values of the buffer at 298 K. The inset shows a plot of emission intensity at 507 nm versus pH. (Excitation $\lambda = 360$ nm.)

Table 6. Selected Bond Lengths (Å) and Angles (deg) for Complex $[Pt(L)(PPh_3)](ClO_4)$ (**3**·ClO_4)

Pt(1)−C(1)	2.005(5)	Pt(1)−N(1)	2.029(5)
Pt(1)−N(2)	2.130(4)	Pt(1)−P(1)	2.242(1)
C(1)−Pt(1)−N(1)	81.02(19)	C(1)−Pt(1)−P(1)	100.58(14)
N(1)−Pt(1)−N(2)	77.00(19)	N(2)−Pt(1)−P(1)	101.81(13)
N(1)−Pt(1)−P(1)	174.07(13)	C(1)−Pt(1)−N(2)	157.41(19)

tentatively assigned to the ^{3}MLCT ($\pi^*(L) \rightarrow d\pi(Pt)$) transition by comparing to the luminescent properties of **1** and **2** as well as its analogous $[Pt(C^N^N)(PPh_3)]^+$. Low-temperature emission spectra of **3** show a remarkable solvent dependent shift of λ_{max} from 496 nm in methanol to 516 nm in acetonitrile (Table 3). The solid-state emission spectrum of **3** at 298 K shows a peak centered at 536 nm, which is consistent with the ligand−ligand interaction observed in the crystal lattice. Similar to that reported in $[Pt(C^N^N)(PPh_3)]^+$, the closest interplanar separation of 3.441(9) Å between two cyclometalating ligands allows overlapping of their π^* orbitals to yield excimeric $\sigma(\pi^*)$ levels and lowers the HOMO−LUMO energy gap.

Effect of Deprotonation of 3·ClO_4. With improved solubility due to the presence of the bulky ancillary PPh_3 ligand, **3**·ClO_4 was selected to demonstrate the pH influence on the photophysical properties of this new class of cycloplatinated system. pH titration was performed in 2:1 DMF/buffered H_2O with a complex concentration of 3×10^{-5} M. At pH < 2.57, complex **3** shows a relatively weak luminescence with λ_{max} located at 504 nm. As shown in Figure 8, changing to a less acidic environment (pH > 4.85) causes a small red-shift of the λ_{max} to 507 nm with a 3-fold enhancement in emission intensity. This red-shift in the emission profile is consistent with the reduction of the MLCT energy gap upon the deprotonation of the 1-pyrazolyl-NH. Previous studies have shown that pyrazolyl anion (pz^-) is a better π-donor than pyrazole (pzH). This destabilizes the $d\pi$ levels of Pt(II) and reduces the $d\pi(Pt) \rightarrow \pi^*(L)$ MLCT energy gap.[15] The red-shift in emission energy is ac-

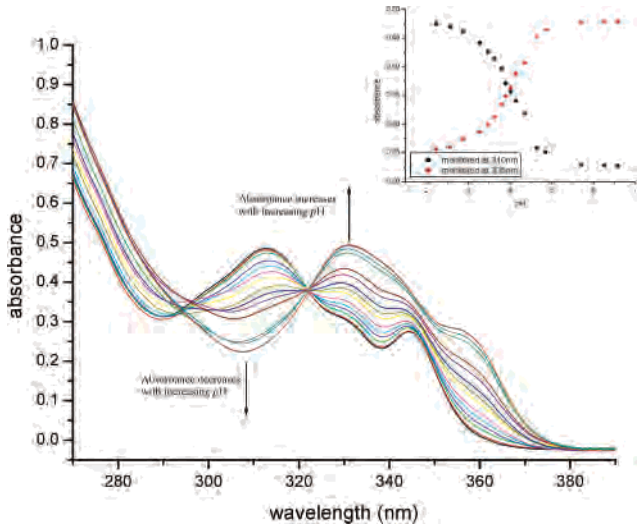

Figure 9. UV−vis absorption spectra of $[Pt(L)(PPh_3)]^+$ (**3**·ClO_4) in 2:1 (v/v) DMF/buffered H_2O (3×10^{-5} M) at different pH values at 298 K. The inset shows a plot of absorbance at 310 and 335 nm versus pH.

companied by a notable enhancement in intensity. This can be rationalized by the destabilization of the high-lying nonemissive d−d excited states upon deprotonation, which reduces their quenching effect on the lower-lying ^{3}MLCT emissive state. The pK_a of **3** is estimated to be 4.0 by monitoring the emission intensity at different pH (inset in Figure 8).

The effect of pH change also leads to a dramatic change in the ground state UV−visible absorption spectra of **3**·ClO_4 (Figure 9). A change of pH from 2.23 to 6.57 results in a continuous red-shift of the absorption bands with a well defined isosbestic point at 322 nm indicating a clean conversion between the protonated and deprotonated forms. The lower energy ^{1}MLCT absorption band shifts from 345 to 355 nm while the higher energy intraligand absorption band shifts from 313 to 331 nm.

Both the pH induced luminescence and the spectroscopic changes of **3** are reversible with alternative addition of triethylamine and trifluoroacetic acid to an acetonitrile solution of **3**. This precludes the possibility that the pH induced photophysical changes of **3** originated from the irreversible formation of the neutral dimer **2**.

Conclusion

In this study, we described the design and synthesis of a novel tridentate C,N,$N_{pyrazolyl}$ cyclometalating ligand, 2-phenyl-6-(1*H*-pyrazol-3-yl)-pyridine (HL), which is able to bring about special structural and spectroscopic features in its cycloplatinated complexes [Pt(L)Cl] (**1**), $[Pt_2(L^-)_2]$ (**2**), and $[Pt(L)(PPh_3)]ClO_4$ (**3**·ClO_4). The versatility of the C,N,$N_{pyrazolyl}$ cyclometalated systems in their ability to respond to pH changes and participate in further chemical functionalization/derivatization is worthy of more in-depth investigations. Work on the functionalization of the C,N,$N_{pyrazolyl}$ cycloplatinated system at the ancillary ligand as well as the 1-pyrazolyl-NH site of the cyclometalating ligand for chemosensing purposes is in progress.

Acknowledgment. The work described in this paper was funded by two grants from City University of Hong Kong (Projects 9610020 and 7001695).

Supporting Information Available: Spectroscopic data and crystallographic data in CIF format for **1**, **2**, and **3**·ClO_4. This material is available free of charge via the Internet at http://pubs.acs.org.

IC062439J